Available online at www.sciencedirect.com

SciVerse ScienceDirect

Ceramics International 38 (2012) 3757–3762

CERAMICS INTERNATIONAL

www.elsevier.com/locate/ceramint

An investigation of the titanium effect on the structural and magnetic properties of $BaNi_2$ based W-type hexaferrites

M.A. Iqbal [a], W. Tahir [a], G. Murtaza Rai [a,*], N.A. Noor [a], Salamat Ali [b], K.T. Kubra [a]

[a] Department of Physics, University of the Punjab, Quaid-e-Azam Campus, Lahore 54590, Pakistan
[b] Department of Physics, G. C. University, Lahore 54400, Pakistan

Received 20 July 2011; received in revised form 5 January 2012; accepted 9 January 2012
Available online 16 January 2012

Abstract

The polycrystalline samples of the composition $Ba(Ni_{1-x}Ti_x)_2Fe_{16}O_{27}$ were prepared by the conventional ceramic method with ($x = 0.0$–1.0). Effects of titanium (Ti) doping on structural and magnetic properties of $BaNi_2$ based W-type hexaferrites were analyzed. The samples were initially sintered in air at 1000 °C for 4 h and finally at 1300 °C for 9 h. The X-ray diffraction patterns confirm the presence of single W-hexagonal phase. The lattice parameters '*a*' and '*c*' were found to show irregular behavior by increasing Ti content. The variations of magnetic properties were observed by analyzing hysteresis loop of prepared samples. The results show that maximum magnetization (M) and remanence (M_r) decrease up to $x \leq 0.6$ due to replacement of Ti ions for spin down ($4f_2$) and spin up (12k, 2a and 2b) sublattices, but a substantial increase of M and M_r for ($x = 0.8$ and1.0) could be attributed to the replacement of Ti ions for spin down sublattices ($4f_2$). The coercivity (H_c) was found to decrease with increasing Ti content. An increase of grain size with Ti content was also observed. Since, H_c is inversely proportional to the packing fraction of magnetic materials or the grain size.

Keywords: C. Magnetic properties; W-Hexaferrite; Diamagnetic substitution; Structure analysis

1. Introduction

Ferrites are magnetic materials containing complex iron oxides with interesting magnetic properties [1]. These are considered to be very important class of materials from applications point of view. Therefore, various efforts have been carried out by the researchers to improve the structural, electrical and magnetic properties. The advantage of ferrites is that they yield higher efficiency and lower costs than that of other materials [2]. They are used in radio and television, microwave and satellite communications. In recent years, the successful applications of ferrimagnetic materials (ferrites) in nearly all important technical fields of modern life have been reported [3]. Snoek, in 1947, obtained ferrites which were very useful at high frequencies [4]. Barium based hexagonal ferrites are ideal filters for electromagnetic interference attenuation purposes due their low cost, high stability and high density [5]. Microwave absorbers are highly demanded in defense and aerospace industries, as the application of microwave-absorbing coating on the exterior surfaces of military aircrafts and vehicles helps to avoid detection by the radar (Stealth technology) [6]. Wave absorbing materials are required to have a large electric and magnetic loss in the frequency range of interest. It has been reported that barium hexagonal ferrites are suitable candidates for high density, over coat free, contact or semi-contact recording media [7]. On account of their superior chemical stability, mechanical hardness, excellent corrosion and wear resistance, and level of media noise, they are also suitable for rigid disk media without protective and lubricant layers. Due to large magneto-crystalline anisotropy and strong dependence of the orientation of easy axis on the microstructure, they have the best potential for application in both perpendicular and longitudinal magnetic recording media [8,9]. Several works have been reported on barium hexaferrites for use as microwave absorption materials.

Hexagonal ferrites are divided into six different types: M ($AFe_{12}O_{19}$), W ($AMe_2Fe_{16}O_{27}$), X ($A_2Me_2Fe_{28}O_{46}$), Y ($A_2Me_2Fe_{12}O_{22}$), Z ($A_3Me_2Fe_{24}O_{41}$), U ($A_4Me_2Fe_{36}O_{60}$),

* Corresponding author. Tel.: +92 42 99239238; fax: +92 42 35856892.
E-mail address: gm_rai786@yahoo.com (G. Murtaza Rai).

0272-8842/$36.00
doi:10.1016/j.ceramint.2012.01.021

where A = Ba, Sr, La and Me = a bivalent transition metal [10]. In these types, mostly W-type barium ferrites are used as electromagnetic wave absorbers [11,12]. The dielectric and magnetic properties such as saturation magnetization, coercivity, resistivity, permeability, etc., can be controlled by substitution of divalent or trivalent ions [13]. The crystal structure and chemistry of W-type hexaferrites are closely related to M-type hexaferrites. The crystal structure of M- and W-type hexaferrite can be described as an alternating stacking of S and R blocks in the direction of hexagonal *c*-axis. The spinel blocks in the W-type structure are twice as thick as the M-structure [14]. A number of investigations have been reported for studying the effect of Ni–Ti doping on electromagnetic wave absorbing and magnetic recording properties of M-type ferrite [15].

In this work, we prepared the single phase NiTi Substituted W-type hexaferrite by ceramic method, and investigated the effects of the $Ni^{2+}Ti^{2+}$ substituted W-type barium ferrites (WBF). The crystalline structure and magnetic properties of the $Ni^{2+}Ti^{2+}$ substituted barium W-type hexaferrites $Ba(Ni_{1-x}Ti_x)_2Fe_{16}O_{27}$ ($x = 0.0$–1.0) prepared by employing conventional ceramic method were studied with a view to study the effect of paramagnetic substitution on the structural and magnetic behavior of ferrites.

2. Experimental

2.1. Powder preparation

Six samples of W-type hexaferrite with compositions, ($BaNi_2Fe_{16}O_{27}$), $BaNi_{1.6}Ti_{0.4}Fe_{16}O_{27}$, $BaNi_{1.2}Ti_{0.8}Fe_{16}O_{27}$, $BaNi_{0.8}Ti_{1.2}Fe_{16}O_{27}$, $BaNi_{0.4}Ti_{1.6}Fe_{16}O_{27}$, $BaTi_2Fe_{16}O_{27}$, were synthesized from stoichiometric amounts of high purity $BaCO_3$ and metal oxides (NiO, TiO and Fe_2O_3) supplied by Riedel-deHaën Laborchemikalien GmbH & Co, KG. The stoichiometric amounts of all raw materials for each sample were weighed by Saratorius Electronic Balance having accuracy up to 10^{-4} g. Each mixture containing raw materials in proper ratio was well mixed for 1.5 h in an agate mortar and pestle to get fine powder. The powder samples were pre-sintered in air at 1000 °C for 4 h in digital furnace (Nabertherm, Model R 60/750) and this sintering was carried out in small steps. The furnace then switched off automatically and slowly cooled down to room temperature. The calcined powder was again ground for an hour to get very fine powder. Powder was then cold pressed at pressure of 49.8 kN for five minutes in Apex Hydraulic Press. The disc-shaped samples were finally sintered in air at 1300 °C for 9 h.

2.2. Characterization

The crystal structure of materials was studied with X-ray diffraction (XRD) on a Bruker D8 Discover diffractometer with Cu Kα radiation in the 2θ range from 10° to 80°. Microstructural analysis of the prepared samples was carried out by S-3400N (HITACHI EMAX) scanning electron microscope. The average grain size was measured directly from the software provided in the machine. Magnetic properties like maximum magnetization (M), remanence (M_r) and coercivity (H_c) for given samples were calculated from the M-H loops at 300 K beginning from zero applied magnetic field to a maximum applied field of (±8000 G). These M-H loops were measured by using Vibrating Sample Magnetometer provided by Lake Shore's new 7400 series.

2.3. Results and discussion

The resulting XRD patterns of the samples of $Ba(Ni_{1-x}Ti_x)_2Fe_{16}O_{27}$ with ($x = 0.0$–1.0) are shown in Fig. 1. By comparing these patterns with JCPDS file 19-0098, it was found that at $x = 0.0$, all the peaks correspond to W-type hexagonal phases. However, a few peaks corresponding to M-type structure at angles (49.5° and 40.9°) were also observed for $x = 0.2$ and $x = 0.6$. This M-type phase was identified by using JCPDF file (27-1029). The presence of M phase can be attributed to the fact that W-type hexagonal ferrites are chemically unstable, some of the W-phases get decomposed to M and α-Fe_2O_3 phases [16,17]. It was reported [18] that unit cell of W-type structure resembles with that of M-type; the only difference is that the successive R-blocks are interplaced by two S-blocks instead one, as in M-phase. The peaks for the Ti doped samples occur at the same positions as for undoped sample but with different intensities. The intensity per reflection for (0 0 12) and (3 0 3) planes increases with Ti content. The decrease of intensity per reflection for (2 0 2) plane is also observed. The peak corresponding to the plane (1 1 10) is not present in samples with $x = 0.0$ and $x = 0.2$, however, it appears as the substitution level is increased to $x > 0.2$. For (1 1 0), (2 0 9) and (2 0 16) planes, the intensity per reflection decreases up to $x = 0.4$ and then diminished as the substitution degree is further increased. This change in relative intensities may be linked with to occupation of the crystallographic sites of the crystal lattice [19]. The lattice parameters a and c were

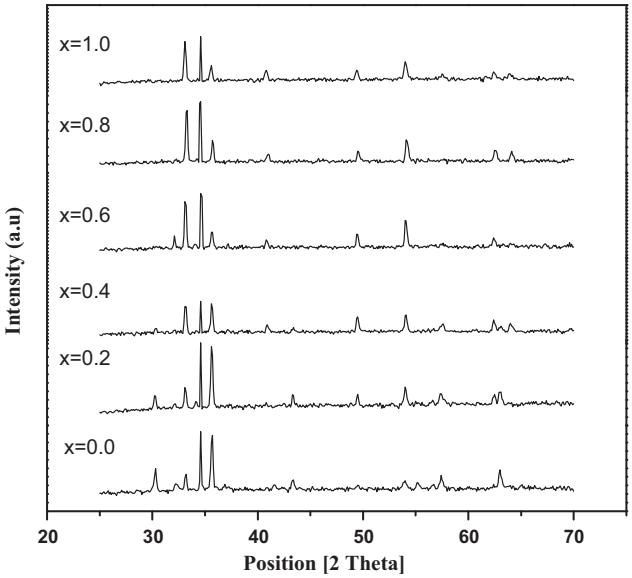

Fig. 1. X-ray diffraction patterns for $Ba(Ni_{1-x}Ti_x)_2Fe_{16}O_{27}$.

calculated by using the formula,

$$\frac{1}{d^2} = \frac{4(h^2 + hk + k^2)}{3a^2} + \left(\frac{l^2}{c^2}\right) \quad (1)$$

where d is the interplanar distance of the lines in the XRD pattern and h, k, l are the related Miller indices. The X-ray density (ρ_x) of the samples is measured by the equation,

$$\rho_x = \frac{2M}{NV} \quad (2)$$

where M represents molar mass, N is Avogadro's number and V is the volume of the unit cell. The cell volume can be calculated by using the following relation,

$$V = a^2 c \sin 120^\circ \quad (3)$$

The values of the above mentioned parameters were calculated by using XRD data of the prepared samples. The calculated values of lattice parameters a (5.89–5.91 Å) and c (32.40–32.84 Å) were found to be in agreement with the literature [20]. The lattice constants c and a of Ti doped samples are greater than those of un-doped samples as shown in Fig. 2. Also, the increase of cell volume with Ti content is remarkable as shown in Fig. 3. These results can be attributed to the fact that ionic radius of Ti^{4+} (1.0 Å) is greater than that of Fe^{3+} (0.64 Å) [21]. The XRD results of our prepared samples of $Ba(Ni_{1-x}Ti_x)_2Fe_{16}O_{27}$ were compared with that of $BaNi_2Fe_{16}O_{27}$ [22] and it was found that with Ti substitution the occurrence of extra phases ($NiFe_3O_4$ and $BaFe_{12}O_{19}$) was eliminated and we get single-phase W-type hexagonal structure with sharp XRD peaks.

Microstructural analysis of the prepared samples was carried out by scanning electron microscopy. SEM micrographs of $Ba(Ni_{1-x}Ti_x)_2Fe_{16}O_{27}$ samples containing titanium contents of $x = 0.0$–1.0 are shown in Fig. 4(a)–(g). It can be seen that for sample with $x = 0.0$, the grains are of irregular shape with average grain size of 11.59 μm. However, by introducing titanium, a trend towards the well defined hexagonal like shape has been observed. In general the grains are of platelet

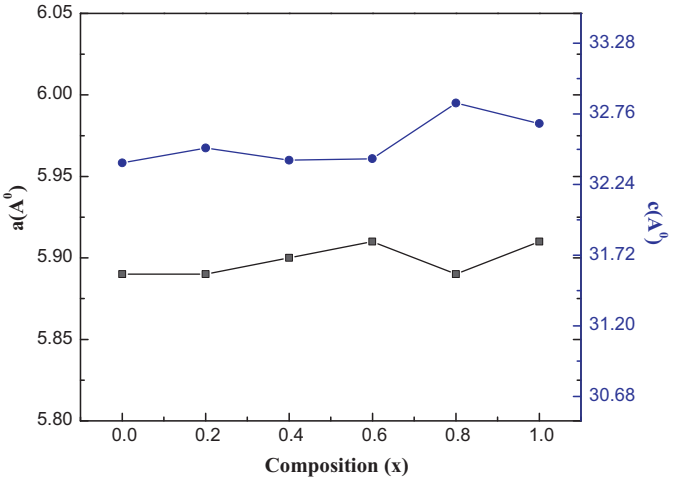

Fig. 2. Dependence on lattice parameters c (Å) and a (Å) with titanium content (x) for $Ba(Ni_{1-x}Ti_x)_2Fe_{16}O_{27}$.

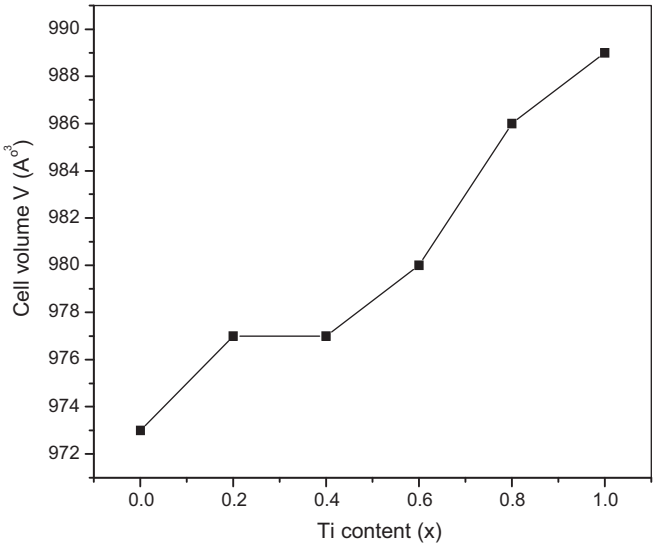

Fig. 3. Variation of cell volume (V) with Ti content (x) for $Ba(Ni_{1-x}Ti_x)_2Fe_{16}O_{27}$.

morphology and some pores are also present in all samples. The variation of the grain size with Ti content (x) is shown in Fig. 5. It is evident that the grain size increases by increasing titanium content (x). It shows that Ti doping contribute to the microstructure change. This also indicates that grain size is the most likely cause of the decreased coercivity observed in doped samples [23].

The magnetic properties may vary with the choice of divalent cations and the way they are distributed among the sub-lattices [24]. Therefore, the effect of titanium doping in $BaNi_2$-W hexaferrite is studied. The magnetic hysteresis loop measurements of the series $Ba(Ni_{1-x}Ti_x)_2Fe_{16}O_{27}$ ($x = 0.0$–1.0), is shown in Fig. 6. Table 1 shows the values of magnetic parameters of these compounds obtained from the data of Fig. 6. In Table 1, we found that the values of maximum magnetization M, and the remnant magnetization M_r, decrease with increasing x values from 0.0 to 0.6. On the contrary, the values of M and M_r increase when $x = 1.0$. The unit cell of W-type hexaferrite crystal structure, being investigated, is built up by the superposition of two spinel and hexagonal blocks, containing Fe^{3+} ions allocated in five different sublattices, namely 12k, $4f_2$, 2a, $4f_1$ and 2b which are distributed in both blocks [25]. Three, of these positions, 12k, $4f_2$ and 2a have octahedral environment, while $4f_1$ shows tetrahedral environment and 2b occupies a pseudo-tetrahedral (bypyramidal) site. Further, $4f_1$ and $4f_2$ have spin down configurations; while other three sites (12k, 2a and 2b) contribute positively to magnetization. Therefore, each magnetic sublattice has a specific contribution to total magnetization. However, the magnetic properties are strongly affected by the substitution of paramagnetic and diamagnetic cations [26,27]. In the series $Ba(Ni_{1-x}Ti_x)_2Fe_{16}O_{27}$ compounds, Ni^{2+} ions are partially replaced by Ti^{4+} ions. Ni^{2+} ion has strong preference for octahedral sites [28]. The substitution of Ti^{4+} ions instead of Ni^{2+} ions located at octahedral sites make some Fe^{3+} ions to migrate from octahedral to tetrahedral sites. The paramagnetic Ti^{4+} ions

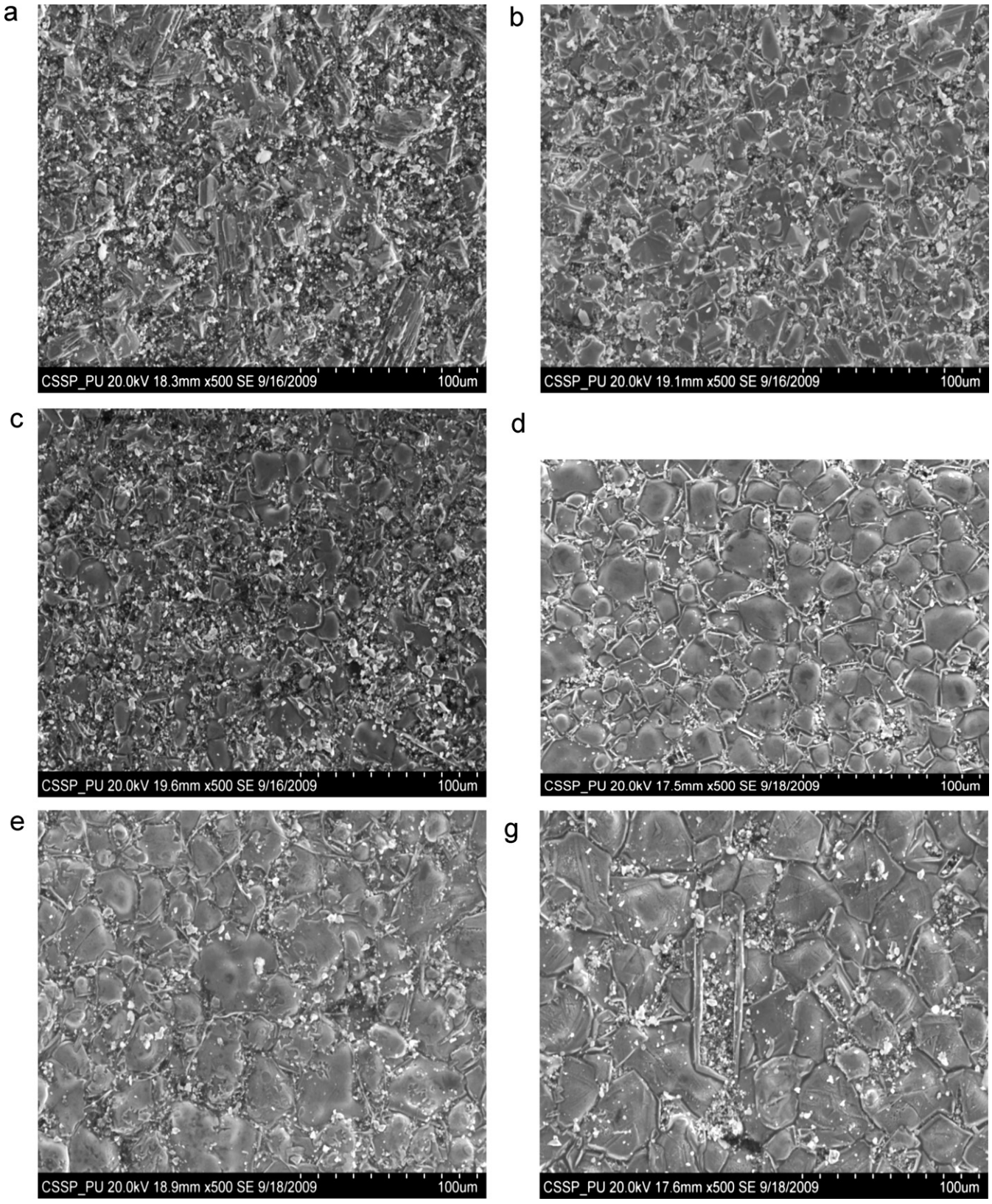

Fig. 4. Scanning electron micrograph of W-type hexagonal $Ba(Ni_{1-x}Ti_x)_2Fe_{16}O_{27}$ with $x = 0.0$.

may occupy the spin up or spin down octahedral sublattices vacated by Fe^{3+} ions [29]. This replacement of Ti^{4+} ions into the octahedral sites is responsible for the variation of net magnetizations of the materials [30].

According to the variation of the maximum magnetization (M) of the series $Ba(Ni_{1-x}Ti_x)_2Fe_{16}O_{27}$ with x values (Table 1), we conclude that when $x \leq 0.6$, Ti^{4+} ions substitute for the spin-down sublattices ($4f_2$) and other octahedral spin-up sublattices

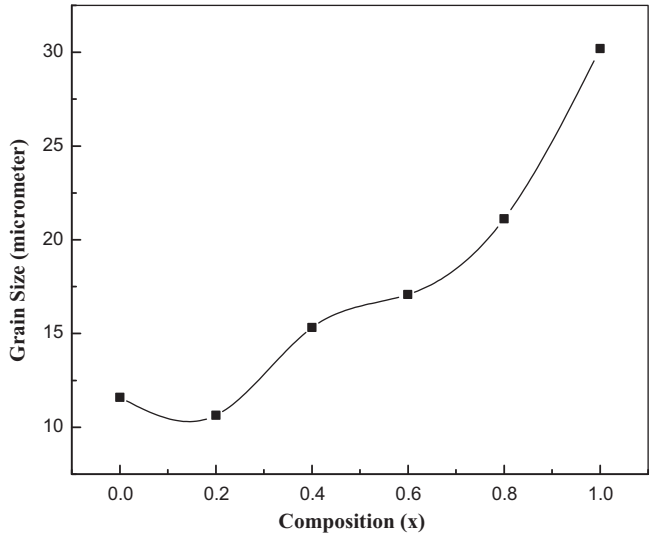

Fig. 5. Dependence of grain size on Ti content for $Ba(Ni_{1-x}Ti_x)_2Fe_{16}O_{27}$.

(12k, 2a and 2b); therefore, the values of M and M_r of compounds decrease with increasing x values. However, the increase of M and M_r, when ($x = 0.8$ and 1.0) can be attributed to the replacement of paramagnetic Ti^{4+} ions into the spin down sublattices $4f_2$ [31,32].

Each loop is clearly indicating low coercivity for each of the composition, showing that all samples belong to soft ferrite family. The variation of coercivity (H_c) with Ti content (x) for Ba $(Ni_{1-x}Ti_x)_2Fe_{16}O_{27}$ are presented in Table 1 and shown in Fig. 7. It is clear that increase in Ti content (x) results in the decrease of coercivity and this behavior can be explained on the basis of site preference of Ti^{4+} ions. Since the $4f_2$ sublattice has a strong influence in coercivity, the preference of Ti^{4+} for this ($4f_2$) site, would contribute to the decrease of coercivity [33]. Moreover, one might think that the 2b sublattice is also actively involved. In practice, change of H_c can be attributed to a particular cation substitution on several Fe^{3+} sites. Moreover,

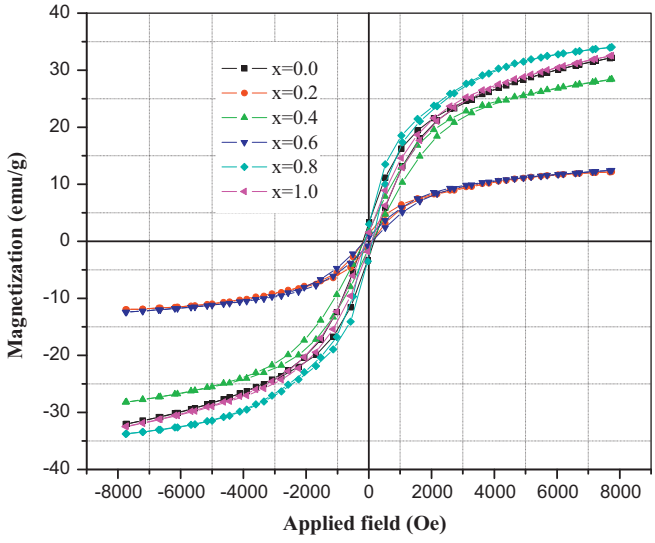

Fig. 6. The hysteresis loops for $Ba(Ni_{1-x}Ti_x)_2Fe_{16}O_{27}$ W-type hexagonal ferrites prepared by ceramic method.

Table 1
Values of H_c, M and M_r for $Ba(Ni_{1-x}Ti_x)_2Fe_{16}O_{27}$ with ($x = 0.0$–1.0).

Sample	Magnetization, M (emu/g)	Retentivity, M_r (emu/g)	Coercivity, H_c (Oe)
$BaNi_2Fe_{16}O_{27}$	32.108	3.159	186
$BaNi_{1.6}Ti_{0.4}Fe_{16}O_{27}$	12.06	1.214	153
$BaNi_{1.2}Ti_{0.8}Fe_{16}O_{27}$	28.31	1.710	148
$BaNi_{0.8}Ti_{1.2}Fe_{16}O_{27}$	12.44	0.765	131
$BaNi_{0.4}Ti_{1.6}Fe_{16}O_{27}$	33.91	2.814	114
$BaTi_2$ $Fe_{16}O_{27}$	32.52	1.809	94

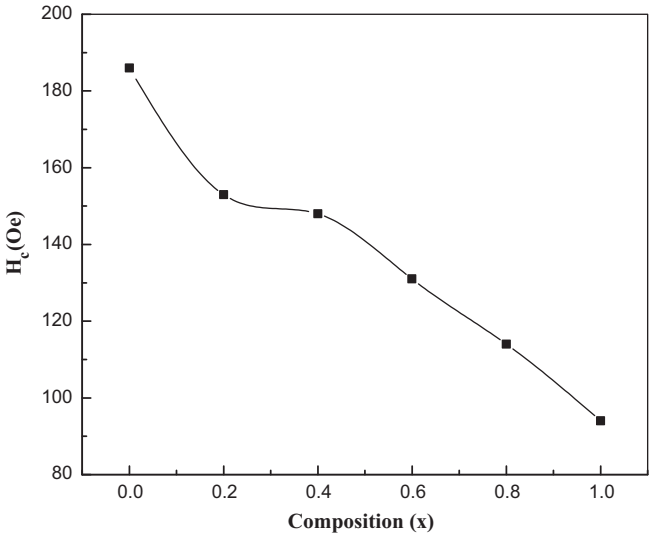

Fig. 7. Dependence of coercivity (H_c) on Ti content (x) for $Ba(Ni_{1-x}Ti_x)_2Fe_{16}O_{27}$.

H_c is inversely proportional to the packing fraction of magnetic materials or the grain size [34]. Our results agree with this correlation because increase in Ti content (x) results in a corresponding decrease of coercivity and increase in grain size [23].

3. Conclusion

The present investigation is mainly devoted to examining the effect of Ti doping on structural and magnetic properties of $BaNi_2$ W-type hexagonal ferrites. The X-ray diffraction patterns confirm that dominant phases are W-hexagonal for all samples. However, in some samples, few extra peaks corresponding to M-type structure were also observed. The lattice parameters c and a show irregular trend by increasing the substitution level of titanium (Ti). The hysteresis loops for all samples are clearly indicating low coercivity, revealing that all the samples belong to the family of soft ferrites. The value of coercivity tends to decrease by increasing the substitution level of paramagnetic titanium (Ti^{4+}) ions. SEM micrographs indicate the presence of well defined hexagonal like grains. An increase of grain size by increasing the substitution degree of Ti content is observed. Hence, Ti doped $BaNi_2$ W-type hexagonal ferrites may be suitable for their applications at higher frequencies and as radar wave absorbing materials.

Acknowledgements

This work was done in the frame of Indigenous Scholarship scheme project. The authors would like to thank the financial support of the Higher Education Commission (HEC) of Pakistan. The authors are grateful to Dr. Saira Riaz (Center for solid state Physics, University of the Punjab, Lahore, Pakistan) for giving us access to magnetic and microstructure measurement facilities. Equally thank to Farooq Bashir (Lahore College for Women University) for his kind help in XRD analysis.

References

[1] A. Goldman, Modern Ferrite Technology, Van Nostrand Reinhold, New York, 1990, pp. 174–200.
[2] A.M. abo El Ata, M.K. El Nimr, D.El. Kony, A.H. Al-Hammadi, Dielectric and magnetic permeability behavior of $BaCo_{2-x}Ni_xFe_{16}$ W-type hexaferrites, J. Magn. Magn. Mater. 204 (1999) 36–44.
[3] B.S. Zlatkov, M.V. Nikolic, O. Aleksic, H. Danninger, E. Halwax, A study of magnetocrystalline alignment in sintered barium hexaferrite fabricated by powder injection molding, J. Magn. Magn. Mater. 321 (2009) 330–335.
[4] J.L. Snoek, New Developments in Ferrimagnetic Materials, Elsevier Publishing Co., Amsterdam, 1947, pp. 16–22.
[5] L. Wang, Q. Zhang, Effect of Fe^{3+}/Ba^{2+} mole ration on the phase format and microwave properties of $BaFe_{12}O_{19}$ prepared by citrate-EOTA complexing method, J. Alloys Compd. 469 (2009) 251–257.
[6] S.M. Abbas, A.K. Dixit, R. Chatterjee, T.C. Goel, Complex permittivity, complex permeability and microwave absorption properties of ferrite polymer composites, J. Magn. Magn. Mater. 309 (2007) 20–24.
[7] N. Matsushita, M.I. Chinose, S. Nagakawa, M. Naoe, Preparation and characteristic of Co–Zn ferrite rigid disks without protective layers for high density recording, IEEE Trans. Magn. 34 (1998) 1639–1641.
[8] Y. Chen, M.H. kryder, Temperature dependent magnetic properties of barium ferrite thin film recording media, IEEE Trans. Magn. 34 (1998) 729–742.
[9] A. Morisako, X. Liu, M. matsumoto, M. Naoe, Effect of underlayer for Ba-ferrite sputtered films on *c*-axis orientation, J. Appl. Phys. 81 (1997) 4374–4376.
[10] J. Smith, H.P.J. Wijin, Ferrites, Philips Technical library, Indhoven, 1959.
[11] M.R. Meshram, N.K. Agrawal, B. Sinha, Characterization of M-type barium hexaferrite-based wide bad microwave absorber, J. Magn. Magn. Mater. 271 (2004) 207–214.
[12] Y. Yang, B.S. Zhang, W.D. Xu, Y. Shi, N. Zhou, H. Lu, Microwave absorption studies of W-hexaferrite prepared by co-precipitation/mechanical milling, J. Magn. Magn. Mater. 265 (2003) 119–122.
[13] A. Ghasemia, A. Hossienpourb, A. Morisako, A. Saatchia, M. Salehi, Electromagnetic properties and microwave absorbing characteristics of doped barium hexaferrite, J. Magn. Magn. Mater. 302 (2006) 429–435.
[14] P.B. .Braun, The crystal structure of a new group of ferromagnetic compounds, Philips Res. Rep. 12 (1957) 491–548.
[15] Xin Tang, Yuanguang Yang, Keao Hu, Structure and electromagnetic behavior of $BaFe_{12-2x}(Ni_{0.8}Ti_{0.7})_xO_{19-0.8x}$ in the 2–12 GHz frequency range, J. Alloys Compd. 477 (2009) 488–492.
[16] F.K. Lotegring, P.H.G.M. Vromans, Chemical instability of metal deficient hexagonal ferrites with W structure, J. Am. Ceram. Soc. 60 (1977) 416–418.
[17] K. Jisheng, L. Huaixian, D. Youwei, W-type hexagonal ferrites $R_xBa_{1-x}Fe_{18}O_{27}$, J. Magn. Magn. Mater. 31 (1983) 801–802.
[18] J. Smith, H.P.J. Wijn, Ferrites, Philips Technical Library, Eindhoven, 1959 , pp. 153–156.
[19] M.J. Iqbal, S. Farooq, Enhancement of electrical resistivity of $Sr_{0.5}Ba_{0.5}Fe_{12}O_{19}$ nanomaterials by doping with lanthanum and nickel, Mater. Chem. Phys. 118 (2009) 308–313.
[20] Y.P. Wu, C.K. Ong, G.Q. Lin, Z.W. Li, Improved microwave magnetic and attenuation properties due to dopant V_2O_5 in W-type barium ferrites, J. Phys. D: Appl. Phys. 39 (2006) 2915–2919.
[21] Y.M. Chiang, D.P. Brinie, W.D. Kingery, Physical Ceramic: Principles for Science and Engineering, John Wiley & Sons, New York, 1997, pp. 323–325.
[22] R. Sharma, R.C. Agarwala, V. Agarwala, A study on the heat treatment of nanocrystalline nickel substituted BaW hexaferrites produced by low combustion synthesis method, J. Magn. Magn. Mater. 312 (2007) 117–125.
[23] I. Bsoul, S.H. Mahmood, A.-F. Lehlooh, Structural and magnetic properties of $BaFe_{12-2x}Ti_xRu_xO_{19}$, J. Alloys Compd. 498 (2010) 157–161.
[24] D.M. Hameda, A. Al-Sharif, O.M. Hameda, Effect of Co substitution on the strucral and magnetic properties of Zn–W hexaferrites, J. Magn. Magn. Mater. 315 (2007) L1–L7.
[25] Z. Haijun, L. Zhichao, M. Chenliang, Y. Xi, Z. Liangying, W. Mingzhong, Preparation and microwave properties of Co- and Ti-doped barium ferrite bycitrate sol-gel process, J. Mater. Chem. Phys. 80 (2003) 129–134.
[26] E. Brando, H. Vincent, O. Dubrinfaut, A. Fourrier-Lamer, R. Lebourgeois, Microwave electromagnetic characteristics of new substituted M-hexaferrites $BaFe_{12-2x}A_xMe_xO_{19}$ (A = Ru, Ir; Me = Co, Zn), J. Phys. IV (France) 7 (1997) 421–422.
[27] C. Wang, L. Li, J. Zhou, X. Qi, Z. Yue, X. Wang, Microstructures and high-frequency magnetic properties of low temperature sintered Co–Ti substituted barium ferrites, J. Magn. Magn. Mater. 257 (2003) 100–106.
[28] A. Goldman, Modern Ferrite Technology, Van Nostrand Reinhold, New York, 1990, pp. 25–29.
[29] A.H. Mones, E. Bank, Cation substitutions in $BaFe_{12}O_{19}$, J. Phys. Chem. Solids 2 (1957) 217–222.
[30] Y.S. Hong, C.M. Ho, H.Y. Hsu, C.T. Liu, Synthesis of nanocrystalline $Ba(MnTi)_xFe_{12-2x}O_{19}$ powders by the sol gel combustion method in citrate acid metal nitrates system (x = 0.0, 0.5, 1.0, 1.5 and 2.0), J. Magn. Magn. Mater. 279 (2004) 401–410.
[31] A. Gruskova, J. Slama, M. Michalikova, I. Toth, J. Lipka, Preparation of substituted barium ferrite powders, J. Magn. Magn. Mater. 101 (1991) 227–229.
[32] X. Battle, X. Obradors, J. Rrodriguez-Carvajal, M. Pernet, M.V. Cabanas, M. Vallet, Cation distribution and intrinsic magnetic properties of Co-Ti doped M-type barium ferrite, J. Appl. Phys. 70 (1991) 1614–1623.
[33] G. Mendoza-Suarez, L.P. Rivas-Vazquez, J.C. Corral-Huacuz, A.F. Fuentes, J.I. Escalante-Garcia, Magnetic properties and microstructure of $BaFe_{11.6-2x}Ti_xM_xO_{19}$ (M = Co, Zn, Sn) compounds, Physica B 339 (2003) 110–118.
[34] R. Müller, Preparation of $BaZn_{2-x}Co_xFe_{16}O_{27}$ W-type hexaferrite powders by the glass crystalline method, J. Magn. Magn. Mater. 120 (1993) 61–63.